

13. Pai, E. F. et al. *Nature* **341**, 209–214 (1989).
 14. Neal, S. E., Eccleston, J. F. & Webb, M. R. *Proc. natn. Acad. Sci. U.S.A.* (in the press).
 15. Jurnak, F. *Science* **230**, 32–36 (1985).
 16. Woolley, P. & Clark, B. F. C. *BioTechnology* **7**, 913–920 (1989).
 17. De Vos, A. M. et al. *Science* **239**, 888–893 (1989).
 18. Gibbs, J. B., Schaber, M. D., Allard, W. J., Sigal, I. S. & Scolnick, E. M. *Proc. natn. Acad. Sci. U.S.A.* **85**, 5026–5030 (1988).
 19. Milburn, M. V. et al. *Science* **247**, 939–945 (1990).
 20. John, J., Sohmen, R., Feuerstein, J., Wittinghofer, A. & Goody, R. S. *Biochemistry* (in the press).
 21. Schlichting, I. et al. *Biochemistry* **29**, 504–511 (1990).
 22. Tong, L., Milburn, M., DeVos, A. M. & Kim, S. H. *Nature* **337**, 90–93 (1989).
 23. Gay, N. J. & Walker, J. E. *Nature* **301**, 262–264 (1983).
 24. Leberman, R. & Egner, U. *EMBO J.* **3**, 339–341 (1984).
 25. Feuerstein, J., Goody, R. S. & Webb, M. R. *J. biol. Chem.* **264**, 6188–6190 (1989).
 26. Deakyne, B. & Allen, J. *Am. chem. Soc.* **101**, 3951–3959 (1979).
 27. Kenyon, G. L. & Reed, G. H. *Adv. Enzym.* **54**, 367–426 (1983).
 28. Szegedi, D. M. E. et al. *Trans Am. crystallogr. Ass.* **24**, 167–172 (1988).
 29. Farber, G. K., Machin, P., Almo, S. C., Petsko, G. A. & Hajdu, J. *Proc. natn. Acad. Sci. U.S.A.* **85**, 112–115 (1988).
 30. Hajdu, J. et al. *Nature* **329**, 178–181 (1987).
 31. Hellmell, J. R. et al. *J. appl. Crystallogr.* **22**, 483–497 (1989).
 32. Brünger, A. T., Kurian, K. & Karplus, M. *Science* **235**, 458–460 (1987).
 33. Jones, T. A. *J. appl. Crystallogr.* **11**, 268–272 (1978).
 34. Pai, E. F. et al. *EMBO J.* (in the press).
 35. Reinstein, J., Schlichting, I. & Wittinghofer, A. *Biochemistry* (in the press).

ACKNOWLEDGEMENTS. We thank Marija Isakov and Anna Scherer for technical assistance, Ken Holmes for support, encouragement and suggestions during the writing of the manuscript, Lynne Howell for help with data reduction, and Greg Farber and Barry Stoddard for help with the Laue experiments. G.A.P. thanks the Alexander von Humboldt Foundation for support. The work was also supported by the European Community.

Deficiency of a glycoprotein component of the dystrophin complex in dystrophic muscle

James M. Ervasti, Kay Ohlendieck, Steven D. Kahl, Mitchell G. Gaver
& Kevin P. Campbell*

Howard Hughes Medical Institute and Department of Physiology and Biophysics, University of Iowa College of Medicine, Iowa City, Iowa 52242, USA

Dystrophin, the protein encoded by the Duchenne muscular dystrophy (DMD) gene, exists in a large oligomeric complex. We show here that four glycoproteins are integral components of the dystrophin complex and that the concentration of one of these is greatly reduced in DMD patients. Thus, the absence of dystrophin may lead to the loss of a dystrophin-associated glycoprotein, and the reduction in this glycoprotein may be one of the first stages of the molecular pathogenesis of muscular dystrophy.

DUCHENNE muscular dystrophy is caused by a defective gene located on the X chromosome. Dystrophin, the high-molecular weight protein product of the DMD gene¹, is localized to the sarcolemmal membrane of normal skeletal muscle^{2–5} but is absent from the skeletal muscle of people with DMD^{1,2,6}, *xmd* dogs⁷ and *mdx* mice^{1,5} (the last two being possible animal models for DMD). The amino-acid sequence of dystrophin suggests that it is a membrane cytoskeletal protein^{8,9} involved in the anchoring of sarcolemmal proteins to the underlying cytoskeleton. But the exact function of dystrophin and its precise role in the resulting necrosis of dystrophic muscle fibres has not been determined. In studies of other genetic diseases involving proteins of the cytoskeleton^{10,11}, the absence of one component is sometimes accompanied by the loss of another cytoskeletal protein. Therefore, to understand the molecular pathogenesis of DMD, we sought to identify the proteins associated with or bound to dystrophin and to characterize the status of these proteins in muscle where dystrophin is absent.

Recently, we have shown that dystrophin can be isolated from detergent-solubilized skeletal muscle membranes using wheat-germ agglutinin (WGA)-Sepharose, because of its tight association with a WGA-binding glycoprotein¹². This indicates that the localization of dystrophin to the cytoplasmic face of the sarcolemma^{2–5} results from a tight association of dystrophin with an integral membrane glycoprotein. Here we report the purification of a large oligomeric complex (~18S) containing

dystrophin using sucrose density-gradient centrifugation in the presence of digitonin. We have identified four glycoproteins of apparent relative molecular masses (M_r) 156,000 (156K), 50K, 43K and 35K as integral components of the dystrophin complex. The 156K and 50K glycoproteins are sarcolemmal glycoproteins, as shown by indirect immunofluorescence. Immunoaffinity beads raised against dystrophin and the 50K glycoprotein selectively adsorb the dystrophin-glycoprotein complex. Furthermore, there is a marked reduction of the 156K glycoprotein in muscle from *mdx* mice and DMD patients. These results imply that in dystrophic muscle, the absence of dystrophin may lead to the loss of a dystrophin-associated glycoprotein. This could be the first step in the molecular pathogenesis of muscular dystrophy.

Dystrophin-glycoprotein complex

This complex was isolated following digitonin-solubilization of rabbit skeletal muscle membranes using WGA-Sepharose and DEAE-cellulose¹² and further purified by sucrose density gradient centrifugation in the presence of 0.1% digitonin. It is evident from the Coomassie blue-stained gel of sequential gradient fractions (Fig. 1a) that the dystrophin-glycoprotein complex was separated from the voltage-sensitive sodium channel and the dihydropyridine receptor (Fig. 1). The size of the dystrophin complex was ~18S in comparison with β -galactosidase (15.9S), thyroglobulin (19.2S) and dihydropyridine receptor (20S) standards. Densitometer scanning of the peak dystrophin-containing fractions (10 and 11, Fig. 1a) revealed several proteins that co-purified with dystrophin: a broad, diffusely staining component with an apparent M_r of 156K, an 88K protein, a triplet of proteins centred at 59K, a 50K protein, a doublet at 43K and proteins of 35K and 25K.

To identify the glycoprotein constituents of the dystrophin-glycoprotein complex, sucrose gradient fractions 7–17 were electrophoretically separated, transferred to nitrocellulose and stained with peroxidase-conjugated WGA (Fig. 1b). Four WGA-binding proteins with apparent M_r of 156K, 50K, 43K and 35K were found to strictly co-purify with dystrophin. All four proteins were also positively stained with peroxidase-conjugated concanavalin A. In addition, the lower M_r component of the 43K protein doublet (Fig. 1a) was also positively stained with concanavalin A (not shown).

The dystrophin-glycoprotein complex was further characterized with antibodies raised against various components of the

* To whom correspondence should be addressed.

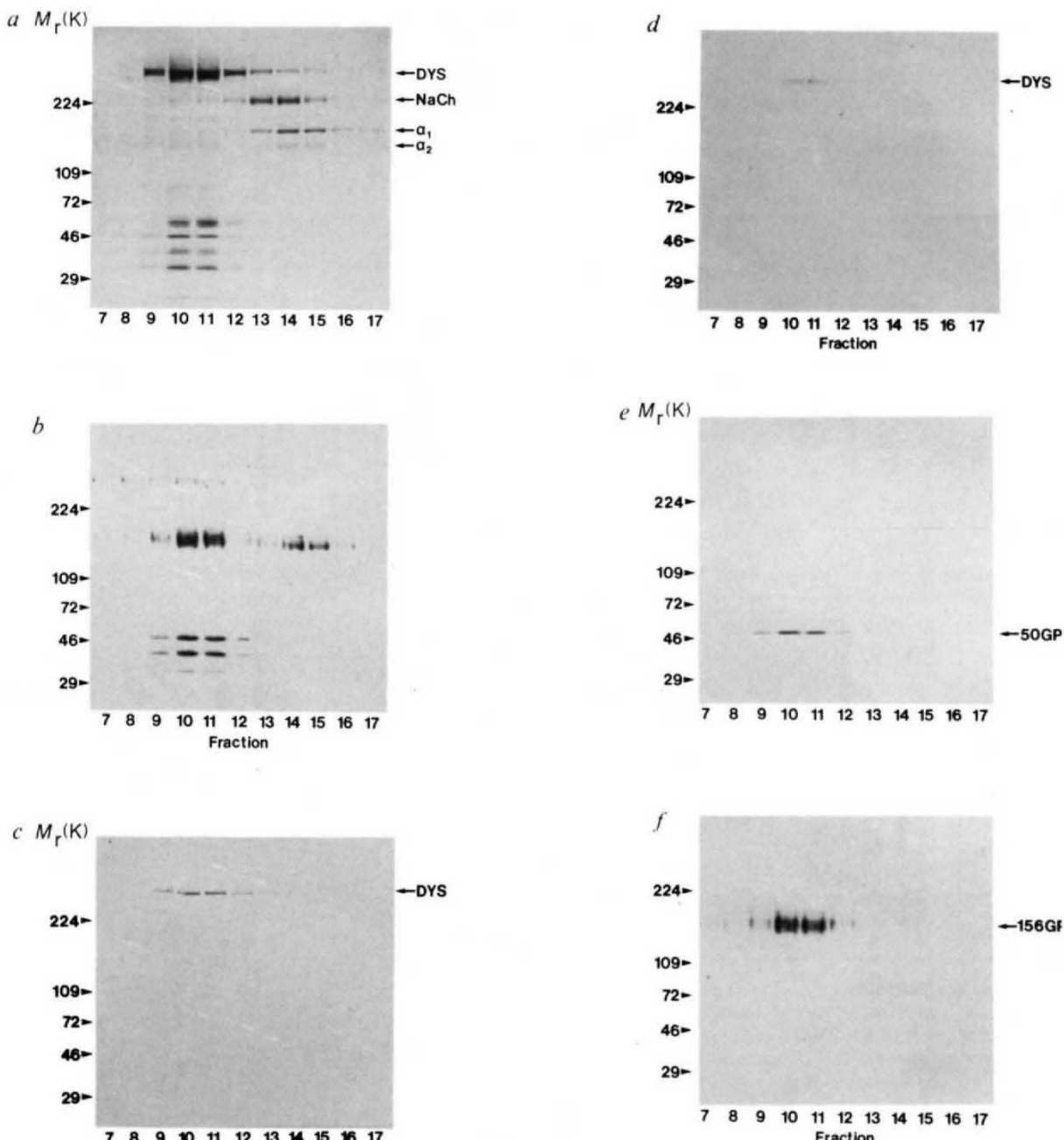


FIG. 1 Sedimentation of dystrophin complex through 5% to 20% linear sucrose gradients. *a*, Coomassie blue-stained gel of sucrose gradient fractions 7-17. *b-f*, Nitrocellulose transfers of sucrose gradient fractions 7-17 separated by SDS-PAGE and stained with: *b*, peroxidase-conjugated WGA ($1\ \mu\text{g ml}^{-1}$); *c*, polyclonal antisera against the C-terminal decapeptide of dystrophin; *d*, monoclonal antibody (mAb) XIXC2 against dystrophin; *e*, mAb IVD3₁ against 50K glycoprotein (50 GP); or *f*, mAb VIA4₁ against the 156K glycoprotein (156 GP). Arrows indicate the positions of dystrophin (DYS), the voltage-sensitive sodium channel (NaCh), and the α_1 and α_2 subunits of the dihydropyridine (DHP) receptor. Arrowheads denote the positions of the molecular weight standards as indicated.

METHODS. Heavy microsomes were prepared from rabbit skeletal muscle²⁵ and washed twice with 0.6 M KCl in 50 mM Tris-HCl (pH 7.4), 0.165 M sucrose, 0.1 mM phenylmethylsulphonyl fluoride and 0.75 mM benzamidine to remove contractile proteins. KCl-washed membranes (1 g) were solubilized in 1.0% digitonin, 0.5 M NaCl, and protease inhibitors as previously described¹². After removal of the ryanodine receptor by immunoaffinity chromatography²⁶, the digitonin-solubilized membranes were circulated overnight on a 40 ml WGA-Sepharose column, washed extensively, then eluted with three column volumes of 0.3 M N-acetylglucosamine. Eluted fractions containing dystrophin were applied to a 3-ml DEAE-cellulose column and sequentially eluted with the following NaCl concentrations in buffer A

(0.1% digitonin, 50 mM Tris-HCl, pH 7.4, 0.75 mM benzamidine, 0.1 mM PMSF): 0, 25, 50, 75, 100, 110 and 175 mM. Sucrose gradients (12.5 ml linear 5-20% sucrose) containing 0.5 M NaCl and 0.01% Na₃ in buffer A were prepared using a Beckman density gradient former. Dystrophin complex, which eluted in fraction 2 (3 ml) from the DEAE-column 175 mM NaCl wash, was concentrated to 0.5 ml in a Centricon-100 (Amicon), layered on a sucrose gradient and overlaid with 0.5 ml of buffer A containing 175 mM NaCl and 0.01% Na₃. Gradients were centrifuged at 4 °C in a Beckman VTi 65.1 vertical rotor for 90 min at 200,000g. Fractions (0.6 ml) were collected from the top of the gradients using an ISCO Model 640 density gradient fractionator. Gradient fractions were separated by SDS-PAGE²⁷ (3-12% gradient gel) and stained with Coomassie blue (300 µl concentrated with a Centricon-100) or transferred to nitrocellulose (75 µl of fractions in *b*, 25 µl in *c* and *d*, and 50 µl in *e* and *f*) and stained with various antibodies. The blot shown in *e* was prepared from a gel run in the absence of reducing agent plus 10 mM N-ethylmaleimide. Gel lanes were scanned with a Hoefer GS 300 scanning densitometer and analysed using GS-360 data analysis software. Polyclonal antisera against a chemically synthesized decapeptide representing the C-terminal of dystrophin was raised in New Zealand white rabbits as described²⁸. Hybridomas were obtained from female BALB/c mice which had been immunized with rabbit skeletal muscle membranes and boosted with WGA eluate²⁹.

complex. Antisera from a rabbit immunized with a chemically synthesized decapeptide representing the predicted C-terminal amino-acid sequence of human dystrophin, stained a single high- M_r protein (Fig. 1c). This protein co-migrated with the predominant isoform of dystrophin stained by sheep polyclonal anti-dystrophin antibodies¹³ (not shown). The antisera showed immunofluorescence staining only on the cell periphery (Fig. 2a), which indicates a restricted localization of dystrophin to the sarcolemma of rabbit skeletal muscle.

A library of monoclonal antibodies against muscle proteins eluted from WGA-Sepharose was also screened for reactivity against components of the dystrophin-glycoprotein complex and by indirect immunofluorescence staining of rabbit skeletal muscle. Of six hybridomas which showed immunofluorescence staining only on the sarcolemma, monoclonal antibodies XIXC2 (Fig. 1d) and VIA4₂ (not shown) were found to stain dystrophin on immunoblots. Both dystrophin monoclonal antibodies are IgM subtypes, and recognized both native and denatured dystrophin. Monoclonal antibody XIXC2 also recognizes the minor lower- M_r isoform of dystrophin which co-purifies with the more abundant isoform (Fig. 1d).

Two of the other sarcolemma-specific monoclonal antibodies were specific for components of the dystrophin-glycoprotein complex (Fig. 1e and 1f). The 50K glycoprotein stained with monoclonal antibody IVD3₁ (Fig. 1e), and has been localized exclusively to the sarcolemmal membrane of rabbit skeletal muscle (Fig. 2c). Monoclonal antibody IVD3₁ recognized only the non-reduced form of the 50K glycoprotein and is not highly cross-reactive. Monoclonal antibody VIA4₁ stained the 156K glycoprotein (Fig. 1f) which co-purified with dystrophin. VIA4₁ recognized the denatured form of the 156K glycoprotein and is highly cross-reactive. It also exhibited weak, but specific immunofluorescent staining of the sarcolemmal membrane (Fig. 2d), consistent with its low affinity for the native 156K glycoprotein. In agreement with the immunofluorescence results, a rabbit membrane preparation greatly enriched in sarcolemmal proteins also showed a substantial enrichment in dystrophin, the 156K and 50K glycoproteins (not shown). Immunofluorescence staining for dystrophin, 50K glycoprotein or the 156K

glycoprotein was equally distributed in fast and slow muscle fibres (not shown).

The association of the dystrophin-glycoprotein complex was also assessed by immunoaffinity adsorption. Immunoaffinity beads were prepared with the monoclonal antibodies XIXC2 (anti-dystrophin) and IVD3₁ (anti-50K glycoprotein) and incubated with the partially purified dystrophin-glycoprotein complex. After pelleting the immunoaffinity beads, the supernatants were removed and the beads were washed extensively. The supernatants and washes were pooled (voids), concentrated, and analysed by SDS-polyacrylamide gel electrophoresis and immunoblotting. The voids from the XIXC2 (anti-dystrophin) and the IVD3₁ (anti-50K glycoprotein) immunoaffinity beads contained no dystrophin, 59K triplet, 50K, 43K doublet or 35K proteins as detected by Coomassie blue staining (Fig. 3a). Both the XIXC2 (anti-dystrophin) and IVD3₁ (anti-50K glycoprotein) immunoaffinity beads quantitatively removed dystrophin from the starting material (Fig. 3c). Analysis of the voids for the 156K (Fig. 3d) and 50K (Fig. 3e) glycoproteins revealed that both the XIXC2 and IVD3₁ immunoaffinity beads selectively adsorbed virtually all of each of these glycoproteins from the voids, whereas the voltage-sensitive sodium channel (Fig. 3b) and the α_1 and α_2 subunits of the dihydropyridine receptor (not shown) remained in the voids. As detected by peroxidase-conjugated WGA (not shown), the 43K and 35K glycoproteins were also adsorbed from the voids. Immunoblots of immunoaffinity beads separated on gels indicated that dystrophin, the 156K and 50K glycoproteins were retained by the beads and not selectively proteolysed (not shown). Initial experiments with monoclonal antibody VIA4₁ (anti-156K glycoprotein) have indicated that it has too low an affinity for the native 156K glycoprotein to be successful in this type of experiment.

Analysis of dystrophic muscle

To investigate whether either of the dystrophin-linked 156K or 50K glycoproteins is affected by the absence of dystrophin, immunoblots of skeletal muscle membranes were prepared from control and *mdx* mice and stained with the various antibodies

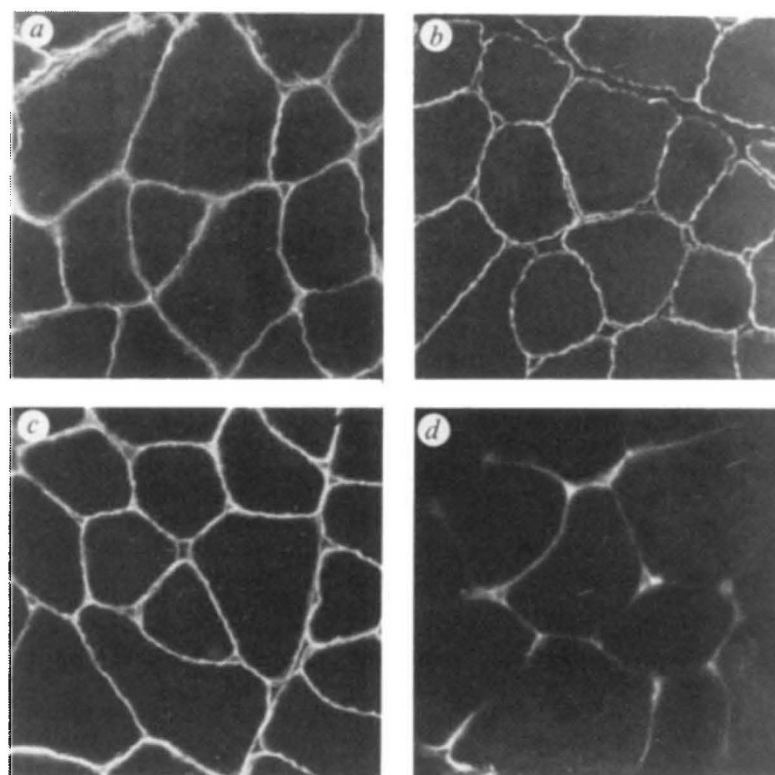
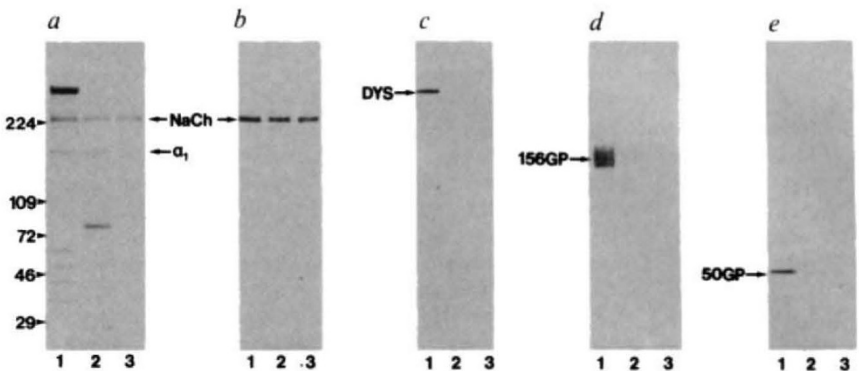


FIG. 2 Immunolocalization of components of the dystrophin complex. Transverse cryostat sections of rabbit skeletal muscle were labelled by indirect immunofluorescence with polyclonal antisera against the C-terminal decapeptide of dystrophin (a), mAb XIXC2 against dystrophin (DYS) (b), mAb IVD3₁ against the 50K glycoprotein (50 GP) (c) and monoclonal antibody VIA4₁ against the 156K glycoprotein (156 GP) (d) (magnification, 250 \times). Staining of the cryostat sections was not observed with nonimmune serum, nor was there any nonspecific binding to the tissue by fluorescein-labelled secondary antibody.

METHODS. The indirect immunofluorescence labelling of fixed 8- μ m transverse cryostat sections from rabbit gastrocnemius was carried out as described²⁹. Sections were pre-incubated for 20 min with 5% normal goat antiserum in PBS buffer, followed by a 2 h incubation at 37 °C with the primary antibody (hybridoma supernatants or 1:1,000 diluted antiserum). After washing in PBS, the sections were further incubated for 30 min at 37 °C in PBS with a 1:50 dilution of FITC-labelled goat F(ab')₂ anti-mouse IgG or anti-rabbit IgG and subsequently examined in a Leitz fluorescence microscope.

FIG. 3 Immunoadsorption of the dystrophin-glycoprotein complex. Fraction 2 (125 µl in *a*, 25 µl in *b*–*e*) eluted from the 175 mM NaCl wash of the DEAE-cellulose column described in Fig. 1 before treatment (lane 1), the XIXC2 affinity column void (125 µl in *a*, 25 µl in *b*–*e*) (lane 2) or the IVD3₁ affinity column void (25 µl) (lane 3), stained with Coomassie blue (*a*), mAb G/C6 against the sodium channel (NaCh) (*b*), polyclonal antisera to the C-terminal decapeptide of dystrophin (DYS) (*c*), mAb VIA4₁ (156 GP) (*d*), or mAb IVD3₁ (50 GP) (*e*). Molecular weight standards (arrowheads) were the same as those used in Fig. 1.

METHODS. Immunoaffinity beads³⁰ were equilibrated with buffer A containing 0.5 M NaCl and then incubated (12 h) with 0.75 ml of fraction 2 from the 175 mM NaCl wash of the DEAE-cellulose column (Fig. 1). After pelleting, the supernatants were decanted (voids) and the affinity beads were washed with 5 aliquots (0.7 ml) of buffer A containing 0.5 M NaCl. The void from each affinity column and the five washes were pooled and concentrated to 375 µl in a Centricon-100. In addition, 0.75 ml of fraction



2 was diluted to 4.2 ml, concentrated to 375 µl and used as control. Column voids were analysed by SDS-PAGE and immunoblotting as described in Fig. 1. Monoclonal antibody G/C6 against the skeletal muscle sodium channel³¹

(Fig. 4). Staining with polyclonal antisera against the C-terminal decapeptide of dystrophin revealed that dystrophin was completely absent from *mdx* mouse membranes (Fig. 4*a*). In addition, comparison of normal and *mdx* mouse with immunostaining by monoclonal antibody VIA4₁ against the 156K glycoprotein revealed that the 156K glycoprotein was absent or greatly reduced in *mdx* mouse membranes (Fig. 4*b*). Staining of identical transfers with sheep polyclonal antisera against either the ryanodine receptor (Fig. 4*c*) or the dihydropyridine receptor (Fig. 4*d*) did not differ between control and *mdx* mouse muscle membranes. Monoclonal antibody IVD3₁ against the 50K glycoprotein did not cross-react with normal mouse membranes and thus could not be evaluated. The absence of the 156K glycoprotein was also confirmed using SDS muscle extracts (not shown) instead of isolated membranes from control and *mdx*

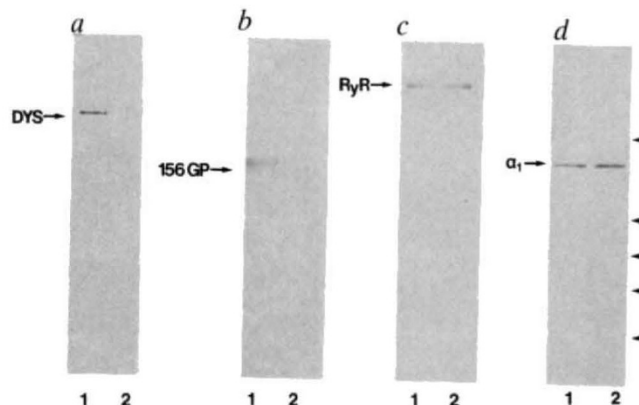


FIG. 4 Immunoblot analysis of control and *mdx* mouse muscle membranes. Immunoblots stained with polyclonal antisera against the C-terminal decapeptide of dystrophin (DYS) (*a*), mAb VIA4₁ against the 156K glycoprotein (156 GP) (*b*), sheep polyclonal anti-ryanodine receptor antibody (RyR) (*c*) and sheep polyclonal anti-DHP receptor antibody (α_1) (*d*) are shown. Lanes (1) and (2) for each panel consist of equal amounts of muscle membrane protein from control and *mdx* mice, respectively (300 µg per lane in (*a*) and (*b*), 150 µg per lane in (*c*) and (*d*)). Molecular weight standards (arrowheads) were the same as Fig. 1.

METHODS. Membranes from control and *mdx* mice (gifts of Dr Richard Strohmen and Dr Richard Entrikin of University of California, Berkeley and Davis, respectively) were prepared in 10% sucrose, 76.8 nM aprotinin, 0.83 mM benzamidine, 1 mM iodoacetamide, 1.1 µM leupeptin, 0.7 µM pepstatin A, 0.23 mM PMSF, 20 mM Tris-maleate, pH 7.0, by centrifuging muscle homogenates for 15 min at 14,000g and subsequently pelleting the supernatant for 30 min at 125,000g followed by KCl washing as described in Fig. 1. Control and *mdx* mouse muscle membranes were analysed by SDS-PAGE and immunoblotting as described in Fig. 1. The amount of 156K glycoprotein in each preparation was estimated densitometrically from autoradiographs of identical blots incubated with ¹²⁵I-labelled sheep anti-mouse secondary antibody³².

mice. Estimation of the amount of 156K glycoprotein remaining in the *mdx* muscle membranes using ¹²⁵I-labelled secondary antibodies and total membrane preparations from four control and four *mdx* mice revealed an average reduction of 85% in *mdx* muscle.

Total muscle extracts were also prepared from biopsy samples of normal controls and DMD patients (obtained from the Department of Neuropathology, University of Iowa). The dystrophic samples showed no staining with antibodies against dystrophin by indirect immunofluorescence microscopy (not shown) and immunoblotting (Fig. 5*a*). In contrast to the normal muscle extract, the three DMD samples showed greatly reduced staining for the 156K glycoprotein (Fig. 5*b*). In contrast, identical immunoblots stained with monoclonal antibodies against the Ca²⁺-dependent ATPase (Fig. 5*c*) revealed no difference in the staining intensity between normal and dystrophic muscle samples. Again, the amount of 156K glycoprotein was reduced by about 90% in DMD samples.

Discussion

We have presented evidence for the existence of a large oligomeric complex (~18S) containing dystrophin, a 59K triplet

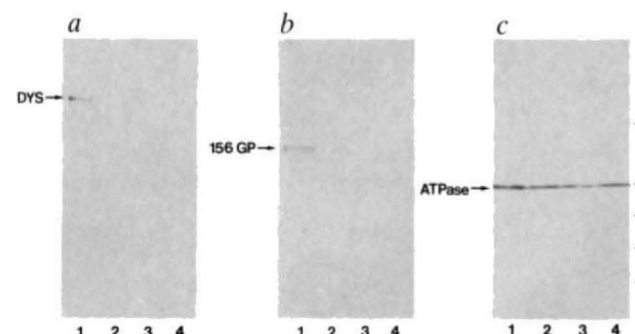


FIG. 5 Immunoblot analysis of normal and dystrophic human muscle biopsies. Immunoblots stained with mAb VIA4₂ against dystrophin (DYS) (*a*), mAb VIA4₁ against the 156K glycoprotein (156 GP) (*b*), or mAb IID8 against the (Ca²⁺+Mg²⁺)-ATPase (ATPase) (*c*) are shown. Lane (1) consists of normal human muscle extract and lanes (2–4) are dystrophic muscle extracts from three DMD patients. Molecular weight standards (arrowheads) were the same as Fig. 1.

METHODS. Frozen muscle biopsy samples (50 mg) were crushed in liquid nitrogen using a mortar and pestle and then prepared for electrophoresis as described⁶. The pulverized muscle samples were transferred to 10 volumes of SDS-PAGE sample buffer (10% SDS, 2 M sucrose, 4% 2-mercaptoethanol, 0.002% bromophenol blue, 260 mM Tris-HCl, pH 6.8), vortexed, and precipitated material allowed to settle. Aliquots (50 µl) of the SDS-extracted muscle samples were analysed by SDS-PAGE and immunoblotting as described in Fig. 1 and the amount of 156K glycoprotein was estimated as described in Fig. 4.

and four sarcolemmal glycoproteins (156K, 50K, 43K and 36K). At least one of the proteins in the complex is an integral membrane protein, as 1.0% digitonin was necessary to solubilize the dystrophin-glycoprotein complex. The immunoaffinity experiments demonstrate that the complex is tightly associated. To date, a large number of antibodies specific for extracellular matrix proteins, cytoskeletal proteins, plasma membrane pump, channel and receptor proteins have been screened for reactivity against the dystrophin-glycoprotein complex. None of these antibodies to known proteins has demonstrated cross-reactivity to any component of the complex. The elucidation of primary sequences by recombinant DNA techniques should provide clues to the function of the dystrophin-associated glycoproteins.

The surface of DMD myofibres have been reported to show altered¹⁴ or decreased¹⁵ lectin binding, and a 370K glycoprotein is apparently missing from DMD muscle¹⁶. However, to our knowledge this is the first demonstration of the marked deficiency of a glycoprotein that is closely linked to dystrophin. The substantial reduction of the 156K glycoprotein from muscles of *mdx* mice and DMD patients is analogous to findings in erythrocytes of individuals afflicted with hereditary elliptocytosis¹⁷, in which the absence of the cytoskeletal protein band 4.1^{11,18,19} is accompanied by greatly diminished steady-state levels of glycophorin C^{10,11}. In both diseases, the disruption of the cytoskeleton seems to destabilize the plasma membrane and

Received 22 December 1989; accepted 26 March 1990.

1. Hoffman, E. P., Brown, R. H. & Kunkel, L. M. *Cell* **51**, 919–928 (1987).
2. Zubrzycka-Gaarn, E. E. *et al.* *Nature* **333**, 466–469 (1988).
3. Arahata, K. *et al.* *Nature* **333**, 861–866 (1988).
4. Bonilla, E. *et al.* *Cell* **54**, 447–452 (1988).
5. Watkins, S. C., Hoffman, E. P., Slayter, H. S. & Kunkel, L. M. *Nature* **333**, 863–866 (1988).
6. Hoffman, E. P. *et al.* *New Engl. J. Med.* **318**, 1363–1368 (1988).
7. Cooper, B. J. *et al.* *Nature* **334**, 154–156 (1988).
8. Koenig, M., Monaco, A. P. & Kunkel, L. M. *Cell* **53**, 219–228 (1988).
9. Davison, M. D. & Critchley, D. R. *Cell* **52**, 159–160 (1988).
10. Alloisio, N. *et al.* *Biochim. biophys. Acta* **816**, 57–62 (1985).
11. Mueller, T. J. & Morrison, M. *Erythrocyte Membrane 2: Recent Clinical and Experimental Advances* 95–112 (Liss, New York, 1981).
12. Campbell, K. P. & Kahl, S. D. *Nature* **338**, 259–262 (1989).
13. Knudson, C. M., Hoffman, E. P., Kahl, S. D., Kunkel, L. M. & Campbell, K. P. *J. biol. Chem.* **263**, 8480–8484 (1988).
14. Bonilla, E., Schotland, D. L. & Wakayama, Y. *Ann. Neurol.* **4**, 117–123 (1978).
15. Capaldi, M. J., Dunn, M. J., Sewry, C. A. & Dubowitz, V. *J. neurol. Sci.* **63**, 129–142 (1984).
16. Capaldi, M. J., Dunn, M. J., Sewry, C. A. & Dubowitz, V. *J. neurol. Sci.* **68**, 225–231 (1985).
17. Palek, J. *Clin. Haematol.* **14**, 45–87 (1985).
18. Alloisio, N., Dorleac, E., Girot, R. & Delaunay, J. *hum. Genet.* **59**, 68–71 (1981).

associated proteins. As antibody probes to other components of the dystrophin complex become available, it will be interesting to determine if any other proteins are also affected in *mdx* and DMD muscle.

How the absence of dystrophin leads to the clinical manifestation of DMD is an unanswered question. Clearly there could be many steps in the disease process, yet we may have identified the first, which is the loss of a dystrophin-associated glycoprotein due to the absence of dystrophin. For example, muscle from *mdx* mice shows elevated intracellular ionized Ca^{2+} levels and corresponding higher net degradation of muscle proteins²⁰. Loss of a dystrophin-anchored protein with a role in the regulation of intracellular calcium could result in elevated intracellular calcium levels and lead to the reported activation of calcium-dependent protease activities²¹. Such a mechanism could explain the abnormal muscle protein degradation and fibre necrosis of dystrophic muscle.

The absence of dystrophin-associated proteins in dystrophic muscle may complicate the therapeutic efficacy of myoblast transfer²², as the reintroduction of dystrophin synthesis might not lead to recovery of associated protein levels and thus could necessitate treatment at only one particular developmental stage. Finally, a deficiency or defect in a dystrophin-associated glycoprotein could perhaps explain the DMD-like symptoms observed in suspected autosomal-recessive patients^{23,24} that express apparently normal dystrophin. □

19. Tchernia, G., Mohandas, N. & Shohet, S. B. *J. clin. Invest.* **68**, 454–460 (1981).
20. Turner, P. R., Westwood, T., Regen, C. M. & Steinhardt, R. A. *Nature* **335**, 735–738 (1988).
21. Nagy, B. & Samaha, F. *J. Ann. Neurol.* **20**, 50–56 (1986).
22. Partridge, T. A., Morgan, J. E., Coulton, G. R., Hoffman, E. P. & Kunkel, L. M. *Nature* **337**, 176–179 (1989).
23. Francke, U., Darras, B. T., Hersh, J. H., Berg, B. O. & Miller, R. G. *Am. J. hum. Genet.* **45**, 63–72 (1989).
24. Zatz, M., Passos-Bueno, M. R. & Rapaport, D. *Am. J. med. Genet.* **32**, 407–410 (1989).
25. Mitchell, R. D., Palade, P. & Fleischer, S. *J. Cell Biol.* **95**, 1008–1016 (1983).
26. Imagawa, T., Smith, J. S., Coronado, R. & Campbell, K. P. *J. biol. Chem.* **262**, 16636–16643 (1987).
27. Laemmli, U. K. *Nature* **227**, 680–685 (1970).
28. Strynadka, N. C. J., Redmond, M. J., Parker, J. M. R., Scraba, D. G. & Hodges, R. S. *J. Virol.* **62**, 3474–3483 (1988).
29. Jorgensen, A. O. *et al.* *Cell Motil. Cytoskel.* **9**, 164–174 (1988).
30. Campbell, K. P. *et al.* *J. biol. Chem.* **262**, 6460–6463 (1987).
31. Casadei, J. M. & Barchi, R. L. *J. Neurochem.* **48**, 773–778 (1987).
32. Sharp, A. H. & Campbell, K. P. *J. biol. Chem.* **264**, 2816–2825 (1989).

ACKNOWLEDGEMENTS. We thank Drs Robert Barchi, Richard Strohmen, Richard Entrikin, Victor Ionasescu and Michael Hart for gifts of antibodies, mice and human tissues used in this study, and William Horne for helpful discussions and Charles Lovig (University of Iowa Cancer Center). K.P.C. is an Investigator of the Howard Hughes Medical Institute. J.M.E. is an NINCDS postdoctoral fellow. This work was supported by the Muscular Dystrophy Association.

LETTERS TO NATURE

Flat-spectrum radio sources: cosmic conspiracy or relativistic neutrons?

Peter M. Giovanoni & Demosthenes Kazanas

Laboratory for High Energy Astrophysics,
NASA/Goddard Space Flight Center,
Greenbelt, Maryland 20771, USA

RADIO-LOUD active galactic nuclei (AGNs) tend to show extended emission in the form of jets and an unresolved central core, from which the jets presumably originate. The intensity spectrum of the core varies smoothly from $10^{8.5}$ to 10^{16} Hz in frequency¹, and is flat (constant with frequency) between 10^9 and 10^{12} Hz, implying that a single emission mechanism, probably synchrotron radiation, is responsible. Because synchrotron emission below $\sim 10^{13}$ Hz would be self-absorbed for a uniform source under conditions typical of AGNs, inhomogeneous models have been used to account for these spectra. These models, which require the magnetic field

strength and the electron density and energy to vary according to strict power laws, reproduce the flat spectra by a number of self-absorbed components^{2–4}, but they do not explain the origin of radiating electrons at $\sim 10^{18}$ cm from the AGN core, in view of the very short lifetime of the electrons in an AGN environment. Here we propose that energy is transported from the central source by relativistic neutrons, which travel freely over a large volume and decay into relativistic protons. The protons produce secondary electrons which generate the observed radiation. The photon spectra thus produced are largely model independent and flat.

Relativistic neutrons can result from the collisions of high-energy protons with the ambient gas⁵, or high-energy protons with the ambient photon field if their energies are sufficiently large⁶. Actually, in high-energy pp collisions the leading particle carries most of the energy⁷. In about half of these interactions the leading proton is converted into a neutron, so the neutrons can carry away $\sim 25\text{--}50\%$ of the total luminosity available (here we assume that this fraction is 25%). But unlike protons, the relativistic neutrons are not tied to the ambient magnetic field; they readily escape from the system and traverse on the average a distance $r \approx 3 \times 10^{13} \gamma_n$ cm before they decay, γ_n being the neutron Lorentz factor. Therefore, if the neutron distribution